

# Broadband $UBVR_CI_C$ Photometry of Horizontal-Branch and Metal-Poor Candidates from the HK and Hamburg/ESO Surveys.

## I.

Timothy C. Beers<sup>1,2,3</sup>

*Department of Physics & Astronomy, CSCE: Center for the Study of Cosmic Evolution,  
and JINA: Joint Institute for Nuclear Astrophysics, Michigan State University, E. Lansing,  
MI 48824*

beers@pa.msu.edu

Chris Flynn<sup>1</sup>

*Tuorla Observatory, Piikkiö, FIN-21500, Finland*

cflynn@astro.utu.fi

Silvia Rossi<sup>1</sup>

*Instituto de Astronomia, Geofísica e Ciências Atmosféricas, Departamento de Astronomia,  
Universidade de São Paulo,  
Rua do Matão 1226, 05508-900 São Paulo, Brazil*

rossi@astro.iag.usp.br

Jesper Sommer-Larsen

*Dark Cosmology Centre, Niels Bohr Institute, University of Copenhagen, Juliane Maries  
Vej 30, DK-2100 Copenhagen, Denmark*

jslarsen@tac.dk

Ronald Wilhelm

*Department of Physics, Texas Tech University, Lubbock, TX 79409*

ron.wilhelm@ttu.edu

Brian Marsteller<sup>2</sup>, Young Sun Lee<sup>2</sup>, Nathan De Lee<sup>2</sup>, Julie Krugler<sup>2</sup>

*Department of Physics & Astronomy, CSCE: Center for the Study of Cosmic Evolution,  
and JINA: Joint Institute for Nuclear Astrophysics, Michigan State University, E. Lansing,  
MI 48824*

marsteller@pa.msu.edu, leeyou25@msu.edu, delee@pa.msu.edu, kruglerj@msu.edu

Constantine P. Deliyannis

*Department of Astronomy, Indiana University, Swain West 409, 727 East Third Street,  
Bloomington, IN 47405*

con@astro.indiana.edu

Franz-Josef Zickgraf<sup>3</sup>

*Hamburger Sternwarte, Universität Hamburg, Gojenbergsweg 112, D-21029 Hamburg,  
Germany*

fzickgraf@hs.uni-hamburg.de

Johan Holmberg<sup>3</sup>

*Max Planck Institute for Astronomy, Koenigstuhl 17, DE-69117 Heidelberg, Germany*

holmberg@mpia.de

Anna Önehag<sup>3</sup>, Anders Eriksson<sup>3</sup>

*Department of Astronomy and Space Physics, University of Uppsala Box 515, SE 751 20  
Uppsala, Sweden*

annao@astro.uu.se, anderse@astro.uu.se

Donald M. Terndrup

*Department of Astronomy, Ohio State University, 140 W. 18th Avenue, Columbus, OH  
43210*

terndrup@astronomy.ohio-state.edu

Samir Salim

*Department of Physics and Astronomy, University of California at Los Angeles, Los  
Angeles, CA 90095*

samir@astro.ucla.edu

Johannes Andersen

*The Niels Bohr Institute, Astronomy, Juliane Maries Vej 30, DK-2100 Copenhagen, Denmark, and Nordic Optical Telescope Scientific Association, Apartado 474, ES-38 700 Santa Cruz de La Palma, Spain*

`ja@astro.ku.dk`

Birgitta Nordström

*The Niels Bohr Institute, Astronomy, Juliane Maries Vej 30, DK-2100 Copenhagen, Denmark, and Lund Observatory, Box 43, S-221 00 Lund, Sweden*

`birgitta@astro.lu.se`

Norbert Christlieb

*Hamburger Sternwarte, Universität Hamburg, Gojenbergsweg 112, D-21029 Hamburg, Germany, and Department of Astronomy and Space Physics, Uppsala University, Box 515, SE-75120, Uppsala, Sweden*

`norbert@astro.uu.se`

Anna Frebel

*Research School of Astronomy & Astrophysics, Australian National University, Cotter Road, Weston, ACT 2611, Australia*

`anna@mso.anu.edu.au`

## ABSTRACT

We report broadband  $UBV$  and/or  $BVR_CI_C$  CCD photometry for a total of 1857 stars in the thick-disk and halo populations of the Galaxy. The majority of our targets were selected as candidate field horizontal-branch or other A-type stars (FHB/A,  $N = 576$ ), or candidate low-metallicity stars ( $N = 1221$ ), from

---

<sup>1</sup>Visiting Astronomer, European Southern Observatory

<sup>2</sup>Visiting Astronomer, WIYN 0.9m. The 0.9m telescope is operated by WIYN Inc. on behalf of a Consortium of ten partner Universities and Organizations (see <http://www.noao.edu/0.9m/general.html>). WIYN is a joint partnership of the University of Wisconsin at Madison, Indiana University, Yale University, and the National Optical Astronomical Observatory.

<sup>3</sup>Visiting Astronomer, Danish 1.5m Telescope

the HK and Hamburg/ESO objective-prism surveys. Similar data for a small number of additional stars from other samples are also reported.

These data are being used for several purposes. In the case of the FHB/A candidates they are used to accurately separate the lower-gravity FHB stars from various higher-gravity A-type stars, a subsample that includes the so-called Blue Metal Poor stars, halo and thick-disk blue stragglers, main-sequence A-type dwarfs, and Am and Ap stars. These data are also being used to derive photometric distance estimates to high-velocity hydrogen clouds in the Galaxy and for improved measurements of the mass of the Galaxy. Photometric data for the metal-poor candidates are being used to refine estimates of stellar metallicity for objects with available medium-resolution spectroscopy, to obtain distance estimates for kinematic analyses, and to establish initial estimates of effective temperature for analysis of high-resolution spectroscopy of the stars for which this information now exists.

*Subject headings:* stars: Population II — stars: early type — stars: horizontal branch — techniques: photometric

## 1. Introduction

Over the course of the past few decades two large objective-prism surveys have enormously expanded the numbers of recognized members of the thick-disk and halo populations of the Galaxy, the HK Survey of Beers and colleagues (Beers, Preston, & Shectman 1985, 1992a; Beers 1999), and the Hamburg/ESO Survey (HES: Wisotzki et al. 1996; Christlieb 2003).

As a result of their great numbers and high luminosities the field horizontal-branch (FHB) stars in these surveys are nearly ideal tracers of the kinematics and dynamics throughout the inner halo ( $R < 20$  kpc) of the Galaxy (e.g., Sommer-Larsen et al. 1997; Wilhelm et al. 1999b). The nearby FHB stars are of particular importance because many of them either already have proper motions available (e.g., UCAC2; Zacharias et al. 2004; USNOB+SDSS; Munn et al. 2004), or they will be measured in the near future (e.g., from ongoing surveys such as the Southern Proper Motion program of van Altena and colleagues, see Girard et al. 2004). When combined with radial velocity information these data allow for refined estimates of the mass of the Galaxy (e.g., Sakamoto, Chiba, & Beers 2003). Also of great interest are the very metal-poor stars from these surveys (stars with metallicities  $[\text{Fe}/\text{H}] \leq -2.0$ , according to the nomenclature of Beers & Christlieb 2005), as they provide crucial elemental abundance information needed to elucidate the nature of the first generations of

stars to form in the Galaxy.

Photometric surveys, such as the ongoing Century Survey Halo project (Brown et al. 2003), searches of the 2MASS Point Source Catalog (Brown et al. 2004), and the Sloan Digital Sky Survey (SDSS: Gunn et al. 1998; York et al. 2000; Yanny et al. 2000; Sirko et al. 2004a,b; Clewley et al. 2005) are providing samples of FHB stars with distances from 5 to more than 100 kpc from the Galactic center. The extension of the SDSS, known as SDSS-II, includes the program SEGUE: Sloan Extension for Galactic Understanding and Exploration. SEGUE will greatly enlarge the list of known distant FHB stars. Given the large range of distances probed by the FHB stars, they provide excellent tools for dynamical determination of the mass distribution of the inner and outer halo (e.g., Sakamoto et al. 2003 and references therein; see also Sirko et al. 2004b), searches for streams of disrupted dwarf galaxies (e.g., Yanny et al. 2000; Newberg et al. 2002; Yanny et al. 2003; Belokurov et al. 2006), and for bracketing estimates of distance to the high-velocity clouds of hydrogen in the Galaxy (e.g., Wakker et al. 1996; Wakker & van Woerden 1997; Wakker 2004; Thom et al. 2006).

Broadband photometry for metal-poor (MP) candidates provides information required to obtain improved metallicities for these stars (in combination with medium-resolution spectroscopy), as well as for the selection of appropriate model atmospheres for analysis of high-resolution spectroscopy (e.g., Cayrel et al. 2004). Accurate distance estimates for the MP stars are needed in order to make full use of available proper motion information to carry out detailed kinematic studies (e.g., Chiba & Beers 2000).

In the color range  $-0.2 \leq B - V \leq 0.4$ , FHB stars have medium-resolution spectra that are quite similar to other A-type stars of higher surface gravity. When analysis of these spectra is combined with measured  $UBV$  colors they can be reliably distinguished (e.g., Wilhelm, Beers, & Gray 1999a). Although it was once thought that the numbers of FHB stars in this color range were likely to dominate the higher surface-gravity stars (e.g., blue stragglers) in the halo of the Galaxy, recent studies have shown that color-selected samples may comprise up to 50% from each of these populations (Norris & Hawkins 1991; Preston, Beers, & Shectman 1994; Wilhelm et al. 1999b; Brown et al. 2004). Finally, we recall that metal-poor main-sequence turnoff (TO) and subgiant (SG) stars in the color range  $0.3 \leq B - V \leq 0.4$  can be distinguished from FHB stars on the basis of their generally higher surface gravities, and its effect on the  $U - B$  color (e.g., Wilhelm et al. 1999a; Bonifacio, Monai, & Beers 2000).

Refinement of the classifications of FHB/A stars is necessary in order to optimize their utility as probes of the Galaxy. The published catalogs of FHB/A candidates from the HK survey (Beers, Preston, & Shectman 1988; Beers et al. 1996; Beers et al. 2006) are certain to comprise a confounded sample, as representatives of both high- and low-surface gravity stars

(as well as outright errors due to mis-classification of prism spectra) are present. The HES contains over 6800 stars that are classifiable as likely FHB stars, some as faint as  $B = 17.5$ . One of our primary reasons for undertaking the photometric study of the FHB/A stars was to test a new method for distinguishing FHB stars from their high-surface gravity counterparts on the basis of the HES objective-prism spectra alone. This new approach makes use of a “Strömgren Index” based on indices obtained directly from the HES prism spectra. Details of this approach, and the results of our tests (using data from the present paper), have been discussed in a separate paper (Christlieb et al. 2005).

In §2 we discuss the selection of stars for inclusion in the present study. The observations and data reduction procedures are presented in §3. The catalog of  $UBVR_CI_C$  photometry is described in §4. For convenience of later use, this information is supplemented by near-infrared  $JHK$  photometry provided by matches to the 2MASS Point Source Catalog (Skrutskie et al. 2006). In §5 we present a brief discussion of the stars contained in the present catalog.

## 2. Sample Selection

Stars for this study were selected for a variety of reasons.

The majority of our candidate FHB/A stars were selected from the HK survey and the HES. A few stars were selected from other sources. These include MP candidates from the HK-II survey of Rhee (2000, 2001), FHB/A candidates from 2MASS, and suspected RR Lyraes from the Robotic Optical Transient Search Experiment (ROTSE-I) Northern Sky Variability Survey (NSVS) catalog (Wozniak 2004), which are being used for an extensive follow-up effort to estimate distances to high-velocity clouds.

The  $UBV$  data we have obtained has been used, in conjunction with available medium-resolution spectroscopy, to assess our ability to uniquely separate the low-gravity FHB stars from the generally higher surface gravity blue straggler and main-sequence A-type stars (Christlieb et al. 2005). The selection of 125 test objects for which we report  $UBV$  photometry in the present paper is described fully by Christlieb et al. (2005). In short, these objects were chosen to cover a range of the approximate Strömgren indices measured from the HES prism plates. These were then used to evaluate the relative success of gravity separation by this approach, by checking their derived classifications with those obtained from the techniques of Wilhelm et al. (1999a). Christlieb et al. (2005) demonstrated that the maximum contamination in samples of HES FHB candidates by higher-gravity A-type stars, when classified via the Strömgren approach, is no more than about 16%.

Our present catalog includes *UBV* photometry for an additional 451 FHB/A candidates that are being used to expand the work of Sommer-Larsen et al. (1997), in order to study the proposed change in the nature of the velocity ellipsoid from the inner to outer halo of the Galaxy. Thom et al. (2005) presents the first results from this ongoing effort.

Some 500 candidate MP stars in our catalog were included because they now have high-resolution spectroscopy available from follow-up studies with 8m-10m class telescopes. Among these programs are the “First Stars” study of Cayrel et al. (2004) with VLT/UVES, and studies of extremely metal-poor stars conducted with Subaru/HDS (e.g., Aoki et al. 2002, 2005, 2006; Honda et al. 2004a,b), and the “0Z” project of Cohen and collaborators (Carretta et al. 2002; Cohen et al. 2002, 2004). A very large sample of high-resolution spectroscopy for over 350 candidate very metal-poor giants with  $[\text{Fe}/\text{H}] \leq -2.0$ , selected primarily from the HES, has recently been reported on by Christlieb et al. (2004) and Barklem et al. (2005). This program, known as the Hamburg/ESO R-process Enhanced Star (HERES) survey, used VLT/UVES to obtain moderate signal-to-noise ( $S/N \sim 30/1 - 50/1$  per pixel),  $R \sim 20000$  spectra in order to identify additional examples of highly r-process-element enhanced stars similar to the well-known stars CS 22892-052 (Snedden et al. 2003) and CS 31082-001 (Cayrel et al. 2001; Hill et al. 2002), as well as to better assess their frequency of occurrence over this metallicity range. Many of these stars were included in our sample selection. A number of the bright metal-poor stars selected by Frebel et al. (2006) for which high-resolution spectroscopy either presently exists, or will soon be obtained, were also included in our observational program.

Numerous stars from the HK and HES surveys exhibit strong CH G-bands, indicative of large carbon abundances (see, e.g., Christlieb et al. 2001; Marsteller et al. 2005; Lucatello et al. 2006). Many (roughly 100) have had high-resolution spectroscopy gathered by a number of groups (e.g., Barklem et al. 2005, Tsangarides et al. 2005; Aoki et al. 2006); these stars were included in our observing program as well.

### 3. Observations and Data Reduction

The photometry observations reported in the present paper were conducted over a total of 28 runs with 6 different telescope/detector combinations during the period 1998 to 2006. There were 13 runs with the ESO/Danish 1.5m telescope on La Silla, 10 runs with the WIYN 0.9m telescope on Kitt Peak, three runs with the CTIO 0.9m (including two conducted by the SMARTS consortium), one run with the CTIO 1.0m (conducted by the SMARTS consortium), and a single run with the Hiltner 2.4m telescope at the MDM observatory on Kitt Peak. Details of the dates of the runs, and the observers who participated in each run,

are listed in Table 1.

### 3.1. The ESO/Danish 1.5m Observations

Observations were obtained with the ESO/Danish 1.5m telescope at the European Southern Observatory using the DFOSC instrument, as described by Brewer & Storm (1999). Prior to September 2000, the C1W7 CCD (a Loral/Lesser backside-illuminated chip with  $15\ \mu\text{m}$  pixels) was employed. After this date a new EEV CCD was installed, with the same pixel size, an improved readout noise ( $3e^-$  vs.  $7e^-$  for the previous chip), and a much higher full-well capacity than the previous chip. In both cases, the ESO  $UBV$  and/or  $BVR_CI_C$  filter sets were employed.

A reasonably clean and uniformly illuminated portion of the full chip was identified, and the program stars were located close to its center. Because we were primarily observing single stars in each pointing, only the central  $250 \times 250$  pixels surrounding the region of interest were read out. Observations were typically taken by running sequences of  $V - B - U - U - B - V$  or  $V - B - R_C - I_C - I_C - R_C - B - V$  filters, with a bias taken after each cycle.

The goal was to set integration times so as to obtain a minimum of 15,000 net counts above sky in each filter, so that the summed observations were at least 30,000 net counts. In the case of particularly faint stars the sequences were repeated until the desired sum was obtained, as best as could be judged at the telescope. This goal was naturally much easier met for the brighter stars. In the case of the fainter stars, required integration times became sufficiently long that one must be concerned about changing sky brightness during the course of the observations. In most all cases the longest individual integration times were set to 20 minutes. As a result (and as reflected in Table 2), the photometric errors for fainter stars grow with increasing apparent magnitude.

Nightsky flatfields were obtained (when possible) at the beginning and end of each night, using the same  $250 \times 250$  pixel region as used for the program stars. In later runs, full-chip flatfields were obtained for use in flatfielding the generally much larger fields containing the standards, so that more standards could be used. The standards we employed were taken from the list of Landolt (1992), supplemented in some cases by the Graham (1982) E-region standards. At least several times (typically 3 to 5 times) per night, observations of 2 or 3 extinction standards were attempted (weather permitting), covering a range in airmass from 1.0 to 2.5. These stars were used to provide an independent check on the airmass terms in the final photometric solutions.



### 3.2. The WIYN 0.9m Observations

Observations were obtained with the WIYN 0.9m telescope on Kitt Peak, using the S2KB CCD mounted at the Cassegrain focus. The detector was a SITe  $2048 \times 2048$  pixel array with a plate scale of  $0.6''/\text{pixel}$ , yielding a field of view of  $20.5' \times 20.5'$ . We employed the standard Harris  $UBV$  and/or  $BVR_CI_C$  filter sets, which well reproduce the properties of the Johnson  $UBV$  and Kron-Cousins  $R_CI_C$  system.

Dome flatfields were obtained during each afternoon preceding the night of observations. Standards were taken from the equatorial list of Landolt (1992). For program stars, a cosmetically clean section of the chip covering  $200 \times 200$  pixels was used. Standards were in general taken using the full chip. The sequence of filters, and the targeted net counts (30,000) were obtained in a manner identical to the procedure employed with the ESO/Danish 1.5m described above.

### 3.3. The CTIO 0.9m / Yale 1.0m Observations

Broadband  $UBV$  and  $BVR_CI_C$  observations were taken with the CTIO 0.9m and Yale 1.0m telescopes. Two runs were obtained during SMARTS queue-mode operation, while one run was conducted in classical mode. In all cases, the detector was a  $2048 \times 2046$  QUAD amplifier CCD with a  $13.6'$  field of view. The CCD has a pixel scale of  $0.396''/\text{pixel}$ . The CCD was operated in the QUAD amplifier mode for all runs.

Dome flatfields were obtained in the afternoon before each observing night. In addition, sky flatfields were taken in the evening to supplement the dome flatfields.

Photometric standard fields were taken from the Landolt (1992) equatorial standard catalog. Standards were taken throughout the nights so that we could characterize air-mass extinction coefficients and changes in atmospheric conditions. Each program star was observed using sequences such as those for the ESO/Danish 1.5m described above. The program stars were always positioned in a cosmetically clean portion of the CCD, using a single amplifier.

### 3.4. The Hiltner 2.4m Observations

$BVR_CI_C$  Observations were obtained with the 2.4m Hiltner Telescope of the MDM Observatory. The detector was the “Echelle” CCD, with a frame scale of  $0.28''/\text{pixel}$ . The central  $512 \times 512$  pixel region of the chip was used. Nightly sky flats were obtained in each

filter.

Photometric standards, taken from the Landolt (1992) equatorial lists, were observed on each night. Atmospheric extinction terms were found for each night; the instrumental color terms were taken as the average throughout the run. For both the standards and the program stars, the normal practice was to take three exposures in  $BVR_CI_C$  at each pointing.

### 3.5. Reductions

The data were reduced using the photometry packages found within IRAF<sup>1</sup>. We employed the packages `ccdproc`, `zerocombine`, and `flatcombine` in order to trim the images and assemble a master bias that was applied to all of the images taken on a given night of each run. Master flats in each filter were then constructed for each filter and applied to the appropriate target fields. The package `phot` was then used to obtain aperture photometry for all of the standard and target stars. In this procedure, a single (typically a 15'' aperture) was defined as the region including the light of the star, and an annulus of 5'' width, located 5'' outside the region of the stellar aperture, was used to estimate the local sky background, which was scaled appropriately and subtracted from the flux included in the stellar aperture.

We then employed the packages `mknobsfile`, `mkconfig`, `fitparams` and `invertfit` to obtain the instrumental magnitudes of the standard stars; these were then used to determine the coefficients for the transformation equations for each magnitude or color. These solutions were then applied to the standard stars to verify their validity before applying them to the target stars to obtain calibrated magnitudes. As a quality check, stars from the various programs were observed on multiple nights during each run, and also across the various telescope/detector combinations. A number of stars were identified from this procedure for which the data appeared less than optimal; these stars are noted in the reported results.

## 4. Results

Although the quality of the photometry obtained varied from telescope to telescope, and from run to run, we have a sufficient number of independently observed stars taken during the program to estimate the scatter obtained over the entire sample. These are listed, as a

---

<sup>1</sup>IRAF is distributed by the National Optical Astronomy Observatories, which is operated by the Association of Universities for Research in Astronomy, Inc. under cooperative agreement with the National Science Foundation.

function of  $V$  magnitude ranges, in Table 2. This Table lists the average one-sigma errors in the measured  $V$  magnitudes and in the optical colors obtained from our observations and reductions. These estimates provide a good picture of the level of (internal) accuracy one can expect for the great majority of stars reported here. The total number of observations involved are listed in the second column of Table 2. The average internal errors are listed in the third column of Table 2, on the lines labeled “INT”. These errors are dominated by photon statistics and residuals in the reduction solutions. As can be seen from inspection of the Table, the typical internal errors range from 0.002 mag to 0.006 mag for the brightest stars, to on the order of 0.02 mag to 0.05 mag for the faintest stars.

In order to obtain an estimate of the typical external errors in our measurements, we have also computed the average one-sigma errors in the measured  $V$  magnitudes and optical colors for stars that were observed across multiple runs, and/or with multiple telescope/detector combinations. The total number of observations involved are listed in the second column of Table 2. The average external errors are listed in the third column of Table 2, on the lines labeled “EXT”. As can be seen from inspection of the Table, the typical external errors range from 0.010 mag to 0.012 mag for the brightest stars, to on the order of 0.027 mag to 0.037 mag for the faintest stars. We conclude that for stars brighter than  $V = 15$ , the external errors of determination in the apparent magnitudes and colors are on the order of 2%, while errors of 3% to 3.5% apply for the stars fainter than  $V = 15$ .

We observed a sufficient number of stars that had previously reported  $UBV$  photometry (see, e.g., Pier 1982; Doinidis & Beers 1990, 1991; Preston, Shectman, & Beers 1991; Beers et al. 1992b; Preston et al. 1994; Norris, Ryan, & Beers 1999; Wilhelm et al. 1999b; Bonifacio et al. 2000), obtained during the course of the HK survey, to obtain an independent comparison. Figure 1 shows a plot of the comparison of the  $V$  magnitudes,  $B - V$ , and  $U - B$  colors for the stars in common. As can be seen in the Figure, the agreement is excellent. From the 185 stars in common between the present and previous samples, we obtain average zero-point offsets of:

$$\begin{aligned} \langle V_{\text{pres}} - V_{\text{prev}} \rangle &= -0.005 \text{ mag} \\ \langle (B - V)_{\text{pres}} - (B - V)_{\text{prev}} \rangle &= +0.005 \text{ mag} \\ \langle (U - B)_{\text{pres}} - (U - B)_{\text{prev}} \rangle &= -0.001 \text{ mag} \end{aligned}$$

The average one-sigma scatter in the different measurements is:

$$\begin{aligned}
\langle \sigma (V_{\text{pres}} - V_{\text{prev}}) \rangle &= 0.026 \text{ mag} \\
\langle \sigma ((B - V)_{\text{pres}} - (B - V)_{\text{prev}}) \rangle &= 0.028 \text{ mag} \\
\langle \sigma ((U - B)_{\text{pres}} - (U - B)_{\text{prev}}) \rangle &= 0.022 \text{ mag}
\end{aligned}$$

In the above expressions “pres” refers to the present sample and “prev” refers to the previous samples.

The great majority of the stars in common have  $V \leq 15$ ; the average one-sigma scatter between the two sets of stars are commensurate with the expected level of external errors listed in Table 2. There were not a large enough number of stars observed across the various telescope/detector combinations to obtain a breakdown of how the zero points and scatter might vary for each of these combinations relative to previously reported photometry. However, sanity checks performed during the course of assembling the results for the small number of previously observed stars did not indicate cause for concern.

Table 3 lists the final results for our program stars. For each star we list the star name, the  $V$  magnitude, the  $B - V$ ,  $U - B$ ,  $V - R_C$ , and  $V - I_C$  colors, along with the one-sigma errors of their determination, and the total number of independent observations obtained for each magnitude or color. Stars for which our repeated measurements indicated that the reported results might be suspect are noted in the Table with a “:” following the reported photometry. This includes a number of stars with extremely red colors (e.g.,  $B - V > 2.5$ ), for which in most cases there was a lack of sufficiently red standards observed during the course of the run to be confident of the resulting solutions.

We have searched the 2MASS Point Source Catalog (Skrutskie et al. 2006) in order to obtain  $JHK$  magnitudes for our program sample. Table 4 summarizes the results of this exercise. This Table lists the star name, equinox 2000 coordinates, Galactic longitude and latitude, the estimated line-of-sight reddening (described below), the 2MASS identification, and the 2MASS magnitudes and associated errors. Note that we were not able to match up some of our program stars, either because they were too faint to be included in the 2MASS catalog, or because the coordinates from the HK survey were not sufficiently accurate to enable a confident identification. Stars for which the 2MASS catalog match indicated that there were possible problems with the reported photometry (due, for instance, to contamination from nearby stars, or other difficulties) are indicated in the Table with a “:” following the reported 2MASS photometry.

The estimated line-of-sight reddening toward each star is obtained from the dust maps

of Schlegel, Finkbeiner, & Davis (1998), which have superior spatial resolution and are thought to have a better-determined zero point than the Burstein & Heiles (1982) maps. In cases where the Schlegel et al. estimate exceeds  $E(B - V)_S = 0.10$  we follow the procedures outlined by Bonifacio et al. (2000) to reduce these estimates by 35%, and obtain the adopted estimate of reddening,  $E(B - V)_A$ .

Tables 3 and 4 are split into five primary categories: (1) stars from the HK survey, (2) stars from the HES, (3) stars from the HK-II sample of Rhee (2000, 2001) and colleagues, (4) stars from the ongoing HVC tracer star sample of York and colleagues, and (5) stars from other sources. Each star is listed in these sections, ordered by its name. The HK and HK-II survey stars are grouped according to their plate number. Table 5 provides a listing of stars we are aware of in our listing that appear in several surveys (“Other Name”) or which have several names (due to overlapping plates) in the HK survey (“Repeat Object”).

## 5. Discussion

Our catalog includes broadband  $UBV$  and/or  $BVR_CI_C$  photometry for a total of 1857 stars, obtained over the course of 28 runs conducted at various telescopes over the past 8 years. The majority of the stars in this catalog ( $N = 1221$ ) were selected as candidate metal-poor candidates from either the HK survey or the Hamburg/ESO survey. The other large category of targets were the candidate FHB/A stars selected from these same surveys ( $N = 576$ ). A smaller number of additional stars were selected either as metal-poor, FHB/A, or RR Lyrae candidates from other surveys, as described in §2 above.

Figure 2a is a histogram of the distribution of  $V$  magnitude for the stars included in this study (not including stars where the photometry was suspect). Figures 2b-2e are similar histograms that indicate the distribution of measured  $B - V$ ,  $U - B$ ,  $V - R_C$ , and  $V - I_C$  for the stars where this information is available. Figures 2f-2h are histograms of the 2MASS  $J - K$ ,  $H - K$ , and  $J - K$  colors for objects that we were able to match to our program sample.

In Figure 3 we show a de-reddened two-color diagram,  $(U - B)_0$  vs.  $(B - V)_0$ , for the entire set of candidates with that information available. Numerous low-metallicity TO stars can be seen in this Figure in the color range  $0.3 \leq (B - V)_0 \leq 0.5$ , as they are displaced upward from the Population I main-sequence relation. The red dashed line indicates the expected location of main-sequence dwarfs with metallicities  $[\text{Fe}/\text{H}] = -4.0$ , according to synthetic colors based on the Kurucz (1993) models. Note that many of the stars with  $(B - V)_0 > 0.5$  are likely to be giants. The solid green line indicates the rough division

between dwarfs that are expected to be on the main sequence and those stars that may be considered likely Blue Metal Poor (BMP; see Preston et al. 1994) or FHB stars. The BMP candidates are located in the region closest to the red dashed line and blueward of the green line, extending to  $(B-V)_0 \sim 0.15$ . Many of the stars in the color range  $-0.2 \leq (B-V)_0 \leq 0.3$  are metal-poor FHB stars (see Beers et al. 1995; Bonifacio et al. 2000). Note that the low surface gravities of FHB stars displace their positions in the two-color diagram to locations that appear consistent with the Population I dwarf line. The bona-fide FHB stars among these candidates cover ranges of distance between a few kpc up to 75 kpc from the Sun, depending on the color.

All of the stars in our program sample have medium-resolution ( $\sim 2 \text{ \AA}$ ) optical spectroscopy available. Many of the most interesting low-metallicity stars in our sample either already have high-resolution spectroscopy available, or will be studied at high-resolution in the near future. Studies of the kinematics of the BMP/FHB stars included in this sample will be reported in due course.

We are thankful to the ESO/Danish 1.5m, WIYN 0.9m, NOAO, and MDM time assignment committees for awards of the significant amounts of telescope time required for this project, and for the patience to await the results. We are also grateful for the excellent support that we received at the telescopes.

T.C.B., Y.L., B.M., and N.D. acknowledge partial support from grants AST 00-98508, AST 00-98549, AST 04-06784, and PHY 02-16783, Physics Frontier Centers/JINA: Joint Institute for Nuclear Astrophysics, awarded by the U.S. National Science Foundation.

J.K. acknowledges partial support from the Honors College at Michigan State University, in the form of a Professorial Assistantship.

C.F. acknowledges partial support from the Danish National Research Foundation and the Carlberg Foundation.

S.R. acknowledges partial support from the Brazilian institutions FAPESP, CNPq and Capes.

C.P.D. acknowledges partial support from grant AST 02-06202, awarded by the U.S. National Science Foundation.

D.T. and S.S. acknowledge partial support from grant AST 02-05789, awarded by the U.S. National Science Foundation, and from the Ohio State Program for the Enhancement of Graduate Studies (PEGS).

J.A. and B.N. thank the Carlsberg Foundation and the Swedish and Danish Natural

Science Research Councils for partial financial support of this work.

N.C. acknowledges partial support from the Deutsche Forschungsgemeinschaft through grants Ch 214/3 and Re 353/44. N.C. is a research fellow of the Royal Swedish Academy of Sciences supported by a grant from the Knut and Alice Wallenberg Foundation.

A.F. acknowledges partial support from grant DP0342613, awarded by the Australian Research Council.

## REFERENCES

- Aoki, W., Norris, J.E., Ryan, S.G., Beers, T.C., & Ando, H. 2002, *ApJ*, 567, 1166
- Aoki, W., Beers, T.C., Christlieb, N., Norris, J.E., Ryan, S.G., & Tsangarides, S. 2006, *ApJ*, submitted
- Aoki, W., Honda, S., Beers, T.C., Kajino, T., Ando, H., Norris, J.E., Ryan, S.G., Izumiura, H., Sadakane, K., & Takada-Hidai, M. 2005, *ApJ*, 632, 611
- Barklem, P.S., Christlieb, N., Beers, T.C., Hill, V., Holmberg, J., Marsteller, B., Rossi, S., & Zickgraf, F.-J. 2005, *A&A*, 439, 129
- Beers, T.C. 1999, in *The Third Stromlo Symposium: The Galactic Halo*, eds. B.K. Gibson, T.S. Axelrod, & M.E. Putman, (San Francisco: ASP), Vol. 165, p. 206
- Beers, T.C. & Christlieb, N. 2005, *ARA&A*43, 531
- Beers, T.C., Preston, G.W., & Shectman, S.A. 1985, *AJ*, 90, 2089
- Beers, T.C., Preston, G.W., & Shectman, S.A. 1988, *ApJS*, 67, 461
- Beers, T.C., Preston, G.W., & Shectman, S.A. 1992a, *AJ*, 103, 1987
- Beers, T.C., Wilhelm, R., Doinidis, S.P., & Mattson, C.J. 1996, *ApJS*, 103, 433
- Beers, T.C., Rossi, S., Norris, J.E., Ryan, S.G., & Shefler, T. 1999, *AJ*, 117, 981
- Beers, T.C., Doinidis, S.P., Griffin, K.E., Preston, G.W., & Shectman, S.A. 1992b, *AJ*, 103, 267
- Beers, T.C., Almeida, T., Rossi, S., Wilhelm, R., & Marsteller, B. 2006, *ApJS*, submitted
- Belokurov, V., et al. 2006, *ApJ*, 642, L137

- Bonifacio, P., Monai, S., & Beers, T.C. 2000, AJ, 120, 2065
- Brown, W.R., Allende Prieto, C., Beers, T.C., Wilhelm, R., Geller, M.J., Kenyon, S.J., & Kurtz, M.J. 2003, AJ, 126, 1362
- Brown, W.R., Geller, M.J., Kenyon, S., Beers, T.C., Kurtz, M.J., & Roll, J.B. 2004, AJ, 127, 1555
- Brewer, J. & Storm, J. 1999, DFOSC User’s Manual
- Burstein, D., & Heiles, C. 1982, AJ, 87, 1165
- Carretta, E., Gratton, R., Cohen, J.G., Beers, T.C., & Christlieb, N. 2002, 124, 481
- Cayrel, R., Hill, V., Beers, T.C., Barbuy, B., Spite, M., Spite, F., Plez, B., Andersen, J., Bonifacio, P., Francois, P., Molaro, P., Nordström, B., & Primas, F. 2001, Nature, 409, 691
- Cayrel, R., Depagne, E., Spite, M., Hill, V., Spite, F., Francois, P., Plez, B., Beers, T.C., Primas, F., Andersen, J., Barbuy, B., Bonifacio, P., Molaro, P., & Nordström, B. 2004, A&A, 416, 1117
- Chiba, M., & Beers, T.C. 2000, AJ, 119, 2843
- Christlieb, N. 2003, Rev. Mod. Astron. 16, 191 (astro-ph/0308016)
- Christlieb, N., Beers, T.C., Barklem, P.S., Bessell, M., Hill, V., Holmberg, J., Korn, A.J., Marsteller, B., Mashonkina, L., Qian, Y.-Z. et al. 2004, A&A428, 1027
- Christlieb, N., Beers, T.C., Thom, C., Wilhelm, R., Rossi, S., Flynn, C., Wisotzki, L., & Reimers, D. 2005, A&A, 431, 143
- Clewley, L., Warren, S.J., Hewett, P.C., Norris, J.E., Wilkinson, M.I., & Evans, N.W. 2005, MNRAS, 362, 349
- Cohen, J.G., Christlieb, N., Beers, T.C., Gratton, R., & Carretta, E. 2002, AJ, 124, 470
- Cohen, J.G., et al. 2004, ApJ, 612, 1107
- Doinidis, S.P., & Beers, T.C. 1990, PASP, 102, 1392
- Doinidis, S.P., & Beers, T.C. 1991, PASP, 103, 973
- Frebel, A., Christlieb, N., Norris, J.E., Beers, T.C., Bessell, M.S., Rhee, J., Fechner, C., Marsteller, B., Rossi, S., Thom, C., Wisotzki, L., & Reimers, D. 2006, ApJ, in press.



- Girard, T.M., Dinescu, D.I., van Altena, W.F., Platais, I., Monet, D., & Lopez, C.E. 2004, *AJ*, 127, 3060
- Graham, J.A. 1982, *PASP*, 94, 244
- Gunn, J.E. et al. 1998, 116, 3040
- Hill, V., Plez, B., Cayrel, R., Beers, T.C., Nordström, B, Andersen, J., Spite, M., Spite, F., Barbuy, B., Bonifacio, P., Depagne, E., Francois, P., & Primas, F. 2002, *A&A*, 387, 560
- Honda, S., Aoki, W., Ando, H., Izumiura, H., Kajino, T., Kambe, E., Kawanomoto, S., Noguchi, K., Okita, K., Sadakane, K. et al 2004a, *ApJS*, 152, 113
- Honda, S., Aoki, W., Kajino, T., Ando, H., Beers, T.C., Izumiura, H., Sadakane, K., & Takada-Hidai, M., 2004b, *ApJ*, 607, 474
- Johnson, H. L. 1966, *ARA&A*, 4, 193
- Kurucz, R. L. 1993, CD-ROM, 15
- Landolt, A.U. 1992, *AJ*, 104, 340
- Lucatello, S., Beers, T.C., Christlieb, N., Barklem, P.S., Rossi, S., Marsteller, B., Sivarani, T., & Lee, Y. 2006, *ApJ*, submitted
- Marsteller, B., Beers, T.C., Rossi, S., Christlieb, N., Bessell, M., & Rhee, J. 2005, *Nuclear Physics A*, 758, 312
- Munn, J.A. et al. 2004, *AJ*, 127, 3034
- Newberg, H.J., et al. 2002, *ApJ*, 569, 245
- Norris, J.E., & Hawkins, M.R.S. 1991, *ApJ*, 380, 104
- Norris, J.E., Ryan, S.G., & Beers, T.C. 1999, *ApJS*, 123, 639
- Pier, J.R. 1982, *AJ*, 87, 1515
- Preston, G.W., Shectman, S.A., & Beers, T.C. 1991, *ApJS*, 76, 1001
- Preston, G.W., Beers, T.C., & Shectman, S.A. 1994, *AJ*, 108, 538
- Rhee, J. 2000, Ph.D. Thesis, Michigan State University

- Rhee, J. 2001, PASP, 113, 1569
- Sakamoto, T., Chiba, M., & Beers, T.C. 2003, A&A, 397, 899
- Schlegel, D.J., Finkbeiner, D.P., & Davis, M. 1998, ApJ, 500, 525
- Sirko, E., Goodman, J., Knapp, G.R., Brinkmann, J., Ivezić, Z., Knerr, E.J., Schlegel, D., Schneider, D.P., & York, D.G. 2004a, AJ, 127, 899
- Sirko, E., Goodman, J., Knapp, G.R., Brinkmann, J., Ivezić, Z., Knerr, E.J., Schlegel, D., Schneider, D.P., & York, D.G. 2004b, AJ, 127, 914
- Skrutskie, M.F., et al. 2006, AJ, 131, 1163
- Snedden, C., Cowan, J.J., Lawler, J.E., Ivans, I.I., Burles, S., Beers, T.C., Primas, F., Hill, V., Truran, J.W., Fuller, G.M., Pfeiffer, B., & Kratz, K.-L. 2003, ApJ, 591, 936
- Sommer-Larsen, J., Beers, T.C., Flynn, C., Wilhelm, R., & Christensen, P.R. 1997, ApJ, 481, 775
- Thom, C., Putman, M.E., Gibson, B.K., Chrostlieb, N., Flynn, C., Beers, T.C., & Wilhelm, R. 2006, ApJ, 638, L97
- Tsangarides, S. 2005, Ph.D. Thesis, Open University
- Wakker, B.P. 2004, Ap&SS, 289, 381
- Wakker, B.P., & van Woerden, H. 1997, ARA&A, 35, 217
- Wakker, B.P., Howk, C., Schwarz, U., van Woerden, H., Beers, T.C., Wilhelm, R., & Danly, L. 1996, ApJ, 473, 834
- Wisotzki, L., Köhler, T., Groote, D., & Reimers, D. 1996, A&A, 115, 227
- Wilhelm, R., Beers, T.C., & Gray, R.O. 1999a, AJ, 117, 2308
- Wilhelm, R., Beers, T.C., Sommer-Larsen, J., Pier, J.R., Layden, A.C., Flynn, C., Rossi, S., & Christensen, P.R. 1999b, AJ, 117, 2308
- Wozniak, P.R. 2004, AJ, 127, 2436
- Yanny, B., et al. 2000, ApJ, 540, 825
- Yanny, B., et al. 2003, ApJ, 588, 824

York, D.G. et al. 2000, AJ, 120, 1579

Zacharias, N., Urban, S. E., Zacharias, M. I., Wycoff, G. L., Hall, D. M., Monet, D. G., &  
Rafferty, T. J. 2004, AJ, 127, 3043

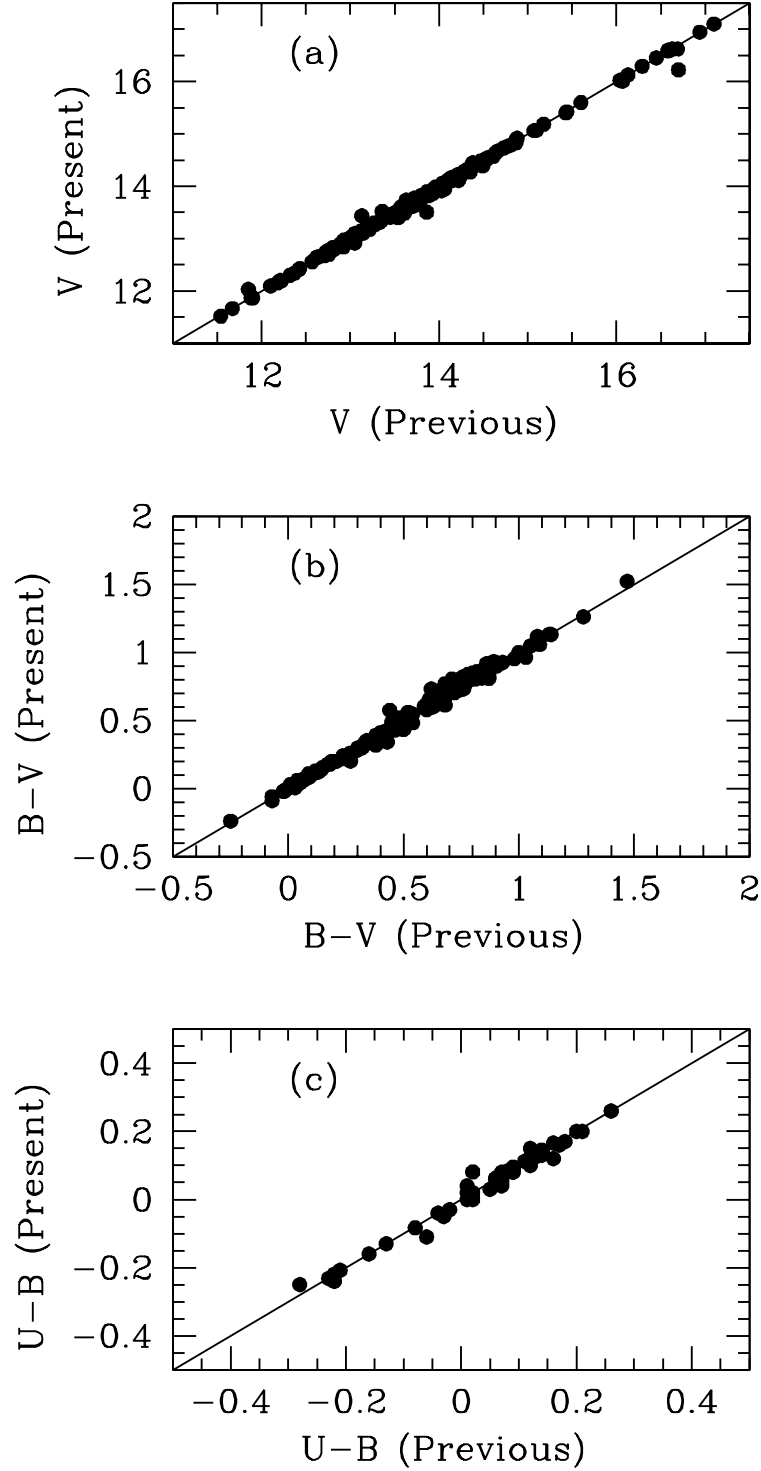


Fig. 1.— Comparison of measured (a)  $V$ , (b)  $B - V$ , and (c)  $U - B$  for stars in the present paper in common with stars having previously reported photometry, from sources listed in the text. The solid line is the one-to-one line. The agreement is excellent.

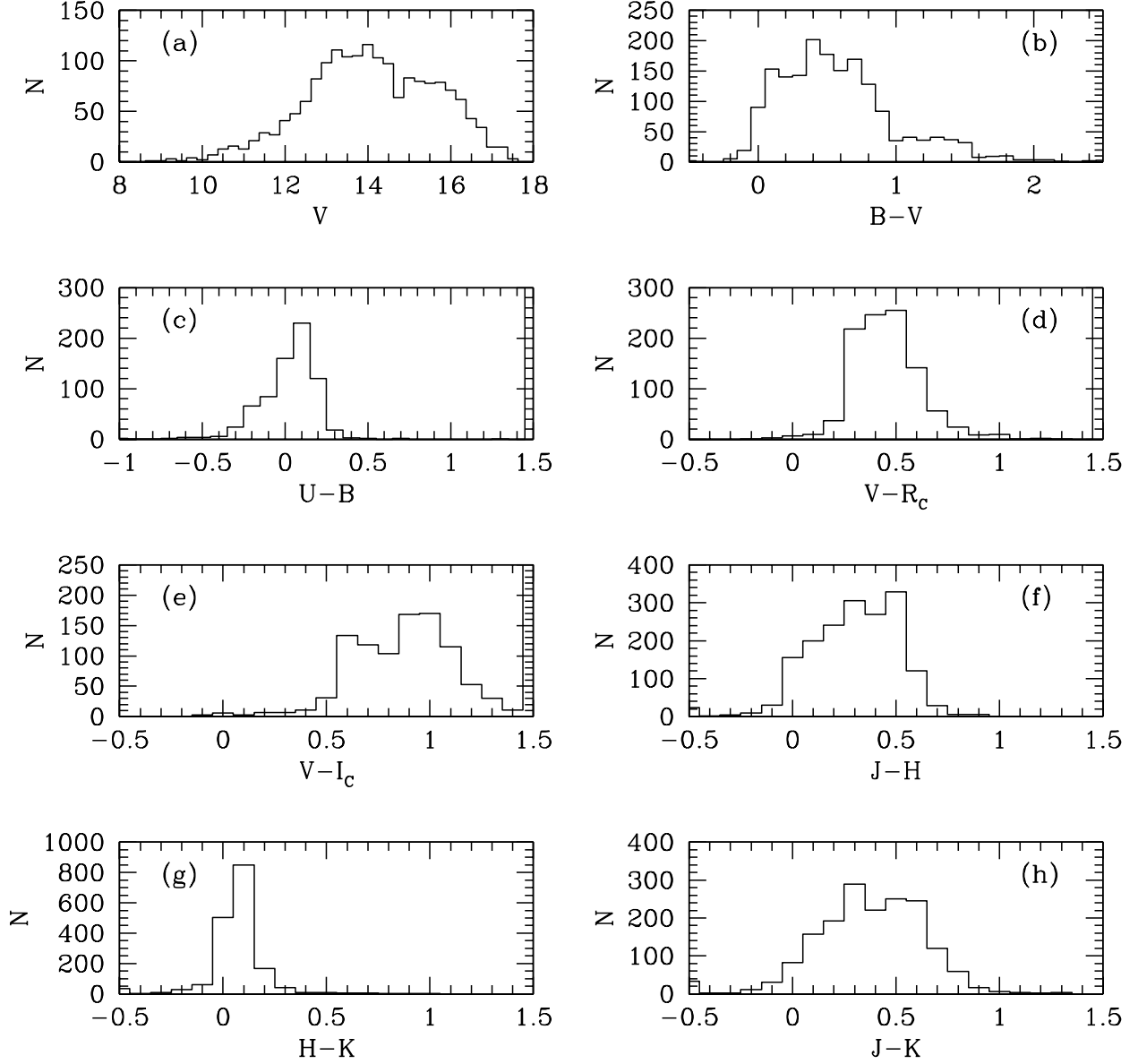


Fig. 2.— (a) Distribution of  $V$  magnitudes for stars in the present sample. Bins are 0.25 magnitudes in width. (b) Similar for  $B - V$  colors. (c) Similar for  $U - B$  colors. (d) Similar for  $V - R_c$  colors. (e) Similar for  $V - I_c$  colors. (f) Similar for  $J - H$  colors. (g) Similar for  $H - K$  colors. (h) Similar for  $J - K$  colors. Bins for the colors are 0.1 magnitudes in width.

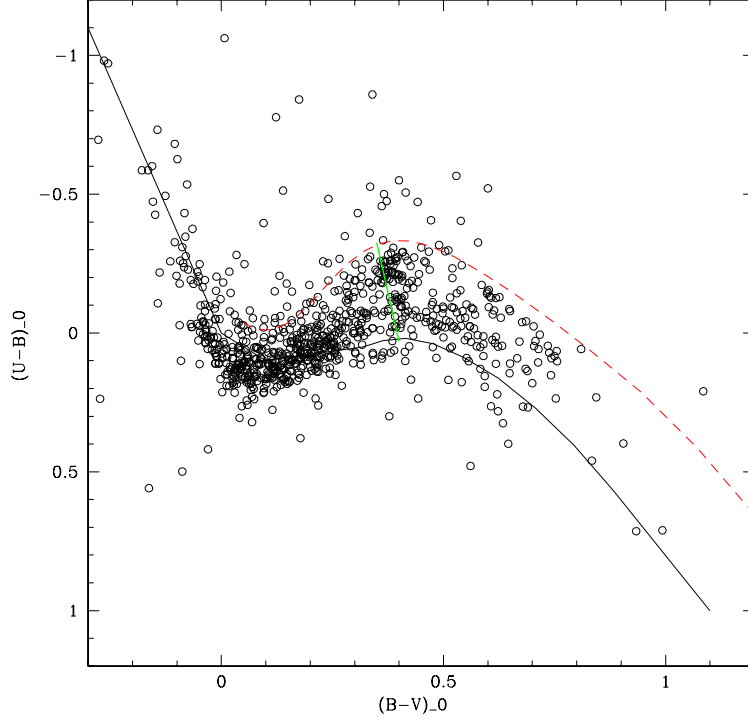


Fig. 3.— De-reddened two-color  $(U - B)_0$  vs.  $(B - V)_0$  diagram for our program stars with this information. The solid line is the Johnson (1966) Population I main-sequence line. The red dashed line is obtained from the predicted  $U - B$  and  $B - V$  colors from the Kurucz (1993) models for main-sequence stars with  $[\text{Fe}/\text{H}] = -4.0$ . The solid green line represents the limit of the expected location of the main-sequence TO for stars of the thick-disk and halo populations. The BMP candidates are located in the region closest to the red dashed line and blueward of the green line, extending to  $(B - V)_0 \sim 0.15$ . Many of the stars in the color range  $-0.2 \leq (B - V)_0 \leq 0.3$  are metal-poor FHB stars. See text for additional comments.

TABLE 1. Log of Observations

Telescope	Dates	Observer
ESO/Danish 1.5m	Nov 1998	C. Flynn
ESO/Danish 1.5m	Nov 2000	T. Beers, S. Rossi
ESO/Danish 1.5m	Jan 2001	T. Beers
ESO/Danish 1.5m	Jun 2001	J. Pritchard
ESO/Danish 1.5m	Dec 2001	T. Beers
ESO/Danish 1.5m	Apr 2002	T. Beers
ESO/Danish 1.5m	Jun 2002	T. Beers
ESO/Danish 1.5m	Oct 2002	J. Holmberg
ESO/Danish 1.5m	Apr 2003	J. Holmberg
ESO/Danish 1.5m	Oct 2003	F.-J. Zickgraf
ESO/Danish 1.5m	Oct 2004	F.-J. Zickgraf
ESO/Danish 1.5m	Nov 2004	A. Önehag, A. Eriksson
ESO/Danish 1.5m	Jan 2006	J. Andersen, B. Nordström
WIYN 0.9m	Sep 2001	T. Beers, B. Marsteller
WIYN 0.9m	Apr 2002	B. Marsteller
WIYN 0.9m	Sep 2002	B. Marsteller
WIYN 0.9m	Jan 2003	B. Marsteller
WIYN 0.9m	Apr 2003	B. Marsteller
WIYN 0.9m	Mar 2004	C. Deliyannis
WIYN 0.9m	Jul 2004	Y. Lee
WIYN 0.9m	Mar 2005	B. Marsteller
WIYN 0.9m	May 2005	Y. Lee, J. Krugler
WIYN 0.9m	Nov 2005	Y. Lee, N. De Lee
CTIO 0.9m	May 2005	SMARTS
CTIO 0.9m	May 2005	N. De Lee
CTIO 0.9m	Jul 2005	SMARTS
CTIO 1.0m	Oct 2005	SMARTS
MDM 2.4m	Oct 2001	S. Salim

TABLE 2. Typical Residuals in Photometry as a Function of  $V$  Magnitude

$V$ Magnitude	N	Error	$\sigma(V)$	$\sigma(B - V)$	$\sigma(U - B)$	$\sigma(V - R_C)$	$\sigma(V - I_C)$
$\leq 11.0$	57	INT	0.002	0.004	0.006	0.006	0.006
	2	EXT	0.012	0.012	0.010	0.013	0.010
11.0 to 11.5	45	INT	0.003	0.005	0.008	0.002	0.003
	5	EXT	0.010	0.015	0.010	0.015	0.012
11.5 to 12.0	63	INT	0.002	0.004	0.008	0.002	0.002
	4	EXT	0.015	0.018	0.015	0.015	0.012
12.0 to 12.5	111	INT	0.003	0.006	0.006	0.003	0.004
	11	EXT	0.019	0.020	0.020	0.018	0.015
12.5 to 13.0	177	INT	0.003	0.005	0.006	0.004	0.004
	21	EXT	0.022	0.020	0.019	0.019	0.016
13.0 to 13.5	230	INT	0.004	0.006	0.007	0.005	0.005
	22	EXT	0.016	0.021	0.023	0.020	0.018
13.5 to 14.0	220	INT	0.004	0.007	0.008	0.005	0.006
	30	EXT	0.013	0.025	0.025	0.022	0.018
14.0 to 14.5	240	INT	0.007	0.011	0.015	0.006	0.006
	31	EXT	0.020	0.026	0.025	0.023	0.019
14.5 to 15.0	173	INT	0.008	0.013	0.016	0.007	0.009
	24	EXT	0.019	0.020	0.026	0.022	0.020
15.0 to 15.5	162	INT	0.010	0.016	0.027	0.007	0.010
	23	EXT	0.025	0.019	0.025	0.023	0.022
15.5 to 16.0	160	INT	0.011	0.018	0.027	0.014	0.018
	28	EXT	0.031	0.035	0.030	0.023	0.025
16.0 to 16.5	119	INT	0.015	0.024	0.041	0.012	0.017
	17	EXT	0.035	0.035	0.031	0.025	0.024
16.5 to 17.0	75	INT	0.020	0.032	0.058	0.037	0.039
	2	EXT	0.037	0.035	0.035	0.030	0.027
$\geq 17.0$	25	INT	0.021	0.033	0.056	0.038	0.040
	0	EXT	...	...	...	...	...



TABLE 3.  $UBVR_CI_C$  Photometry for Program Stars

STAR	$V$	$\sigma(V)$	N	$B-V$	$\sigma(B-V)$	N	$U-B$	$\sigma(U-B)$	N	$V-R_C$	$\sigma(V-R_C)$	N	$V-I_C$	$\sigma(V-I_C)$	N
HK Survey Stars															
BS 15621-047	13.735	0.012	1	0.880	0.019	1	...	...	0	0.504	0.016	1	0.992	0.018	1
BS 15622-017	13.712	0.005	2	0.627	0.010	2	-0.502	0.018	2	...	...	0	...	...	0
BS 15624-067	13.040	0.002	4	0.662	0.003	4	...	...	0	0.297	0.002	4	0.708	0.002	4
BS 15624-094	13.833	0.005	2	0.908	0.008	2	...	...	0	0.335	0.006	2	0.734	0.006	2
BS 15625-001	12.580	0.002	4	0.611	0.004	4	0.027	0.005	4	...	...	0	...	...	0
BS 16023-011	14.302	0.002	4	0.536	0.002	4	-0.016	0.005	2	...	...	0	...	...	0
BS 16023-046	14.170	0.001	6	0.378	0.002	6	-0.231	0.003	6	...	...	0	...	...	0
BS 16033-008	13.786	0.002	4	0.630	0.003	4	...	...	0	0.419	0.003	4	0.843	0.003	4
BS 16033-081	13.347	0.001	6	0.782	0.003	6	...	...	0	0.496	0.002	6	0.988	0.002	6
BS 16034-032	15.468	0.013	1	0.231	0.019	1	0.120	0.035	1	...	...	0	...	...	0
BS 16034-064	14.156	0.004	2	0.603	0.007	2	0.162	0.015	2	...	...	0	...	...	0
BS 16034-090	13.870	0.003	5	0.265	0.004	5	0.052	0.007	5	...	...	0	...	...	0
BS 16034-150	12.136	0.002	2	0.244	0.003	2	0.103	0.004	2	...	...	0	...	...	0
BS 16034-160	13.282	0.009	1	0.566	0.011	1	...	...	0	0.322	0.008	1	0.638	0.008	1
BS 16076-003	13.300	0.006	2	0.710	0.010	2	0.123	0.019	2	...	...	0	...	...	0
BS 16076-006	13.520	0.002	4	0.560	0.004	4	...	...	0	0.405	0.004	4	0.814	0.003	4
BS 16077-004	14.095	0.002	2	0.736	0.004	2	...	...	0	0.423	0.004	2	0.791	0.004	2
BS 16077-030	13.826	0.002	2	0.462	0.004	2	...	...	0	0.290	0.004	2	0.579	0.004	2
BS 16077-045	14.087	0.002	2	0.513	0.003	2	...	...	0	0.343	0.003	2	0.681	0.004	2
BS 16077-046	14.125	0.002	2	0.572	0.004	2	...	...	0	0.359	0.004	2	0.688	0.004	2
BS 16077-051	13.912	0.001	2	0.474	0.002	2	...	...	0	0.308	0.003	2	0.609	0.003	2
BS 16077-054	13.876	0.002	2	0.664	0.004	2	...	...	0	0.424	0.004	2	0.850	0.004	2
BS 16077-056	14.157	0.002	2	0.613	0.004	2	...	...	0	0.359	0.004	2	0.709	0.004	2
BS 16077-058	14.424	0.001	2	0.523	0.002	2	...	...	0	0.335	0.003	2	0.660	0.004	2
BS 16077-068	13.875	0.002	2	0.391	0.004	2	-0.204	0.004	2	...	...	0	...	...	0
BS 16077-070	14.162	0.003	1	0.133	0.005	1	...	...	0	0.462	0.005	1	0.977	0.005	1
BS 16077-072	13.985	0.003	1	0.191	0.005	1	...	...	0	0.483	0.004	1	0.991	0.005	1
BS 16077-076	13.783	0.003	1	0.016	0.005	1	...	...	0	0.425	0.004	1	0.870	0.005	1
BS 16077-077	11.952	0.001	2	0.452	0.001	2	...	...	0	0.293	0.001	2	0.656	0.001	2
BS 16077-080	13.656	0.002	2	0.027	0.004	2	...	...	0	0.428	0.004	2	0.911	0.004	2
BS 16077-088	14.190	0.004	1	0.204	0.006	1	...	...	0	0.503	0.006	1	1.031	0.006	1
BS 16077-091	14.444	0.005	1	0.100	0.008	1	...	...	0	0.468	0.007	1	0.954	0.008	1
BS 16079-006	14.303	0.004	1	-0.127	0.005	1	-0.209	0.007	1	...	...	0	...	...	0
BS 16079-007	13.864	0.003	1	0.501	0.005	1	-0.022	0.013	1	...	...	0	...	...	0
BS 16079-008	13.373	0.003	1	0.419	0.005	1	-0.084	0.010	1	...	...	0	...	...	0
BS 16079-012	14.459	0.005	1	0.411	0.008	1	-0.184	0.019	1	...	...	0	...	...	0
BS 16079-014	13.953	0.004	1	0.277	0.006	1	-0.259	0.010	1	...	...	0	...	...	0
BS 16079-015	13.062	0.003	2	0.076	0.004	2	-0.072	0.007	2	...	...	0	...	...	0
BS 16079-041	14.486	0.005	2	0.572	0.009	2	0.039	0.019	2	...	...	0	...	...	0
BS 16079-044	14.254	0.006	2	0.432	0.010	2	-0.061	0.017	2	...	...	0	...	...	0
BS 16080-036	12.481	0.004	2	-0.027	0.005	2	...	...	0	0.014	0.006	2	0.107	0.007	2
BS 16080-051	13.778	0.004	2	0.605	0.007	2	0.067	0.015	2	...	...	0	...	...	0
BS 16080-052	13.405	0.003	2	0.502	0.005	2	-0.045	0.013	2	...	...	0	...	...	0
BS 16080-053	11.586	0.003	2	1.267	0.007	2	1.287	0.052	2	...	...	0	...	...	0
BS 16080-054	12.776	0.003	3	0.774	0.004	3	...	...	0	0.491	0.003	3	0.990	0.003	3
BS 16080-061	13.566	0.004	2	0.562	0.007	2	0.080	0.014	2	...	...	0	...	...	0
BS 16080-062	14.085	0.004	2	0.624	0.007	2	0.042	0.013	2	...	...	0	...	...	0
BS 16080-081	14.114	0.004	3	0.534	0.007	3	0.002	0.018	3	...	...	0	...	...	0
BS 16080-083	12.772	0.003	1	0.682	0.005	1	0.169	0.008	1	...	...	0	...	...	0
BS 16080-084	14.042	0.007	1	0.470	0.012	1	-0.057	0.015	1	...	...	0	...	...	0
BS 16080-169	14.383	0.019	2	0.539	0.029	2	-0.022	0.041	2	...	...	0	...	...	0
BS 16080-175	14.269	0.003	3	0.491	0.005	3	...	...	0	0.283	0.005	3	0.597	0.005	3
BS 16082-129	13.483	0.001	4	0.731	0.002	4	...	...	0	0.470	0.002	4	0.942	0.002	4
BS 16083-172	13.434	0.002	5	0.624	0.003	5	...	...	0	0.409	0.003	5	0.840	0.003	5
BS 16084-160	13.144	0.003	3	0.858	0.005	3	...	...	0	0.514	0.004	3	1.041	0.003	3

Notes to Table 3.

Table 3 is published in its entirety in the electronic edition. A portion is shown here for guidance regarding its form and content.

TABLE 4. Coordinates and 2MASS  $JHK$  Photometry

STAR	RA (2000) DEC		$l$	$b$	$E(B - V)_A$	2MASS ID	$J$	$\sigma(J)$	$H$	$\sigma(H)$	$K$	$\sigma(K)$
HK Survey Stars												
BS 15621-047	10:09:35.7	+25:59:32	205.3	+54.0	0.030	10093496+2559273	11.955	0.021	11.434	0.019	11.277	0.019
BS 15622-017	12:53:46.1	+23:20:05	311.0	+86.2	0.027	12534619+2320036	12.289	0.020	11.858	0.023	11.799	0.019
BS 15624-067	16:29:01.0	+45:02:58	70.5	+43.5	0.008	16290106+4503007	11.858	0.023	11.485	0.021	11.411	0.019
BS 15624-094	16:17:34.8	+44:08:21	69.5	+45.6	0.014	16173483+4408260	12.675	0.026	12.258	0.026	12.227	0.026
BS 15625-001	11:41:08.9	+27:10:41	208.7	+74.4	0.021	11410898+2710395	11.398	0.027	11.089	0.029	11.021	0.020
BS 16023-011	13:54:20.2	+24:22:49	25.5	+75.6	0.013	13541997+2423008	13.233	0.024	13.033	0.027	12.999	0.035
BS 16023-046	14:00:54.6	+22:46:48	21.3	+73.7	0.017	14005447+2246423	13.241	0.024	13.016	0.027	12.964	0.034
BS 16033-008	13:05:56.1	+25:10:17	2.7	+86.2	0.016	13055616+2510161	12.317	0.024	11.866	0.029	11.803	0.020
BS 16033-081	13:19:12.4	+22:27:57	357.9	+82.2	0.013	13191246+2227575	11.665	0.025	11.158	0.028	11.070	0.024
BS 16034-032	15:35:33.1	+57:53:33	91.5	+48.0	0.012	...	...	...	...	...	...	...
BS 16034-064	15:40:08.4	+57:51:01	91.0	+47.5	0.010	15400798+5751041	13.000	0.024	12.680	0.031	12.654	0.026
BS 16034-090	15:46:44.7	+57:32:51	90.0	+46.8	0.013	15464445+5732527	13.349	0.022	13.235	0.029	13.163	0.035
BS 16034-150	15:39:07.6	+57:49:50	91.1	+47.6	0.012	15390731+5749525	11.491	0.019	11.372	0.029	11.315	0.025
BS 16034-160	15:57:49.6	+56:44:51	88.1	+45.8	0.017	15575051+5644443	12.199	0.022	11.832	0.026	11.817	0.020
BS 16076-003	12:49:26.7	+21:15:28	298.4	+84.1	0.044	12492663+2115234	11.834	0.026	11.351	0.028	11.278	0.019
BS 16076-006	12:48:22.7	+20:56:41	296.3	+83.8	0.031	12482275+2056440	12.123	0.022	11.753	0.029	11.655	0.019
BS 16077-004	11:36:01.8	+31:15:54	194.3	+73.1	0.021	11360176+3115493	12.819	0.029	12.427	0.031	12.347	0.026
BS 16077-030	11:41:54.1	+31:51:15	191.4	+74.2	0.022	11415399+3151128	12.877	0.021	12.632	0.025	12.593	0.027
BS 16077-045	11:46:41.5	+30:46:52	194.6	+75.4	0.023	11464144+3046478	12.994	0.023	12.695	0.021	12.639	0.026
BS 16077-046	11:46:28.2	+31:13:04	193.0	+75.3	0.024	11462812+3113024	13.006	0.027	12.688	0.032	12.634	0.022
BS 16077-051	11:48:29.1	+32:13:57	188.7	+75.4	0.018	11482913+3213584	12.950	0.022	12.641	0.021	12.603	0.023
BS 16077-054	11:48:25.4	+29:54:12	197.9	+75.9	0.017	11482531+2954076	12.409	0.022	11.957	0.028	11.923	0.022
BS 16077-056	11:49:16.1	+28:44:52	202.6	+76.2	0.024	11491616+2844490	12.978	0.021	12.701	0.031	12.611	0.022
BS 16077-058	11:49:07.7	+27:34:47	207.5	+76.2	0.025	11490761+2734455	13.388	0.024	13.114	0.029	13.090	0.030
BS 16077-068	11:51:15.3	+31:23:55	191.3	+76.2	0.020	11511539+3123537	12.978	0.024	12.749	0.021	12.736	0.027
BS 16077-070	11:54:31.1	+31:48:38	188.8	+76.8	0.020	11543096+3148390	12.928	0.023	12.584	0.024	12.562	0.025
BS 16077-072	11:54:11.5	+30:28:46	194.6	+77.0	0.015	11541145+3028437	12.723	0.021	12.371	0.018	12.302	0.022
BS 16077-076	11:53:39.4	+28:35:54	203.0	+77.2	0.023	11533954+2835533	12.710	0.022	12.440	0.023	12.402	0.021
BS 16077-077	11:55:16.6	+28:21:02	204.1	+77.5	0.027	11551655+2821009	10.999	0.022	10.710	0.022	10.652	0.018
BS 16077-080	11:56:10.3	+28:31:05	203.2	+77.7	0.026	11561020+2831066	12.551	0.022	12.254	0.022	12.224	0.020
BS 16077-088	11:55:13.7	+31:07:04	191.6	+77.1	0.017	11551367+3107034	12.875	0.022	12.584	0.023	12.488	0.022
BS 16077-091	11:55:22.4	+31:41:51	189.1	+77.0	0.023	11552238+3141536	13.285	0.026	12.958	0.026	12.881	0.028
BS 16079-006	15:45:37.5	+58:08:12	90.9	+46.7	0.012	15453751+5808130	14.286	0.028	14.345	0.041	14.500	0.087
BS 16079-007	15:44:43.0	+58:00:09	90.8	+46.9	0.012	15444296+6058091	12.648	0.021	12.317	0.019	12.250	0.023
BS 16079-008	15:44:11.6	+57:53:11	90.7	+47.0	0.013	15441159+5753136	12.159	0.020	11.848	0.021	11.796	0.023
BS 16079-012	15:47:48.1	+57:40:24	90.1	+46.6	0.012	15474803+5740242	13.296	0.021	12.899	0.022	12.874	0.029
BS 16079-014	15:48:28.8	+57:50:17	90.3	+46.5	0.011	15482882+5750160	12.948	0.022	12.657	0.022	12.659	0.028
BS 16079-015	15:47:47.6	+58:06:45	90.7	+46.5	0.012	15474752+5806464	12.752	0.019	12.720	0.022	12.662	0.027
BS 16079-041	15:49:45.9	+58:18:18	90.8	+46.1	0.010	15494570+5818169	13.421	0.025	13.099	0.025	13.097	0.033
BS 16079-044	15:50:04.5	+57:45:24	90.0	+46.3	0.018	15500466+5745204	13.399	0.021	13.164	0.025	13.056	0.036
BS 16080-036	16:36:01.5	+59:44:33	89.8	+40.1	0.021	16360160+5944411	12.181	0.021	12.041	0.021	11.981	0.021
BS 16080-051	16:40:42.8	+60:58:02	91.1	+39.2	0.022	16404266+6058036	12.656	0.022	12.413	0.023	12.319	0.023
BS 16080-052	16:39:32.9	+61:00:18	91.2	+39.3	0.025	16393290+6100177	12.461	0.023	12.214	0.026	12.185	0.022
BS 16080-053	16:39:33.2	+60:53:36	91.1	+39.4	0.032	16393312+6053435	9.427	0.032	8.563	0.031	8.515	0.023
BS 16080-054	16:39:18.5	+60:57:42	91.2	+39.4	0.032	16391853+6057426	11.097	0.023	10.632	0.023	10.508	0.018
BS 16080-061	16:42:52.9	+60:35:16	90.6	+39.0	0.043	16425310+6035149	12.400	0.025	12.119	0.033	12.046	0.028
BS 16080-062	16:41:14.4	+60:39:32	90.7	+39.2	0.047	16411441+6039306	12.815	0.023	12.508	0.026	12.411	0.025
BS 16080-081	16:45:31.3	+60:39:46	90.6	+38.7	0.030	16453149+6039458	13.059	0.027	12.798	0.033	12.704	0.033
BS 16080-083	16:45:07.8	+60:55:53	90.9	+38.7	0.033	16450760+6055491	11.549	0.025	11.270	0.030	11.185	0.023
BS 16080-084	16:46:03.2	+61:10:22	91.2	+38.5	0.033	16460307+6110284	13.094	0.027	12.883	0.034	12.830	0.031
BS 16080-169	16:46:07.1	+60:39:58	90.5	+38.6	0.033	16460717+6040033	13.175	0.022	12.847	0.031	12.842	0.033
BS 16080-175	16:51:08.9	+57:12:25	86.0	+38.7	0.027	16510881+5712277	13.235	0.023	12.977	0.024	12.960	0.030
BS 16082-129	13:47:11.5	+28:57:46	44.7	+77.6	0.015	13471172+2857471	11.855	0.022	11.402	0.021	11.309	0.016
BS 16083-172	14:50:41.6	+48:45:14	84.2	+58.4	0.026	14504144+4845136	11.990	0.021	11.574	0.018	11.496	0.019
BS 16084-160	16:28:50.7	+54:37:03	83.5	+42.2	0.009	16285078+5437067	11.345	0.021	10.838	0.021	10.747	0.018

Notes to Table 4.

Table 4 is published in its entirety in the electronic edition. A portion is shown here for guidance regarding its form and content.

TABLE 5. Other Names and Repeat Objects

STAR	Other Name	Repeat Objects	
BS 15624–067	II 15624–06030		
BS 16023–046		BS 15623–062	BS 16554–041
BS 16033–081		BS 16479–035	
BS 16034–090		BS 16079–013	
BS 16034–150		BS 16086–118	
BS 16077–077		BS 16081–010	
BS 16082–129	II 22881–01863	BS 16078–085	
BS 16086–119			
BS 16467–062		BS 16934–060	
BS 16469–075		BS 16923–089	
BS 16477–003		CS 30317–084	
BS 16479–037		BS 16033–082	BS 16543–058
BS 16543–068		BS 16479–046	
BS 16929–035		BS 16938–053	
BS 17136–013		BS 17448–011	
BS 17136–015		BS 17448–012	
BS 17571–087		BS 17585–121	
BS 17572–100			
CS 22166–022	HE 0926–0508	CS 31065–014	
CS 22172–002	HE 0311–1046		
CS 22185–007	HE 0315–1528		
CS 22189–009	HE 0239–1340		
CS 22874–038	II 22874–01705		
CS 22886–042		CS 29512–051	
CS 22937–087		CS 30492–126	
CS 22952–015	HE 2334–0604		
CS 29493–090	HE 2156–3130		
CS 29502–042		CS 29516–041	
CS 29510–054		CS 29528–025	
CS 29512–030		CS 22886–003	
CS 29512–076		CS 22886–069	
CS 29516–021		CS 29502–007	
CS 29516–023		CS 29502–026	
CS 29520–002		CS 29529–105	
CS 29520–018		CS 29529–116	
CS 30301–152		CS 30325–101	
CS 30301–153		CS 30325–099	
CS 30317–033		BS 16477–044	
CS 30333–062		CS 29522–064	
CS 30333–113		CS 29522–094	
CS 30337–097	HE 2158–3112		
CS 31060–058		CS 29517–043	
CS 31061–022		CS 31063–026	
CS 31061–032		CS 31063–035	
CS 31061–057		CS 31061–057	
CS 31063–025		CS 31074–066	
CS 31070–080		CS 31069–100	
CS 31076–086		CS 31072–104	
CS 31076–119		CS 31072–135	
CS 31078–018		CS 31079–028	
CS 31081–049	HE 0111–1454		
CS 31081–059		CS 31089–062	
CS 31089–081		CS 31090–099	